Journal of Electrical and Computer Engineering Innovations
(JECEI)
Journal homepage: http://www.jecei.sru.ac.ir

SRTTU

JECEI

PAPER TYPE

Image Registration Based on Sum of Square Difference Cost Function

J. Khosravi, M. Shams Esfand Abadi, R. Ebrahimpour*

Faculty of Electrical Engineering, Shahid Rajaee Teacher Training University, P.O. Box: 16785-163, Tehran, Iran.

Article Info

Article History:
Received 24 September 2017
Revised 08 January 2018
Accepted 15 May 2018

Keywords:
Image registration
Sum of square difference
Root mean square error
Mutual information

*Corresponding Author's Email Address:
rebrahimpour@srttu.edu

Extended Abstract

Background and Objectives: There are numerous applications for image registration (IR). The main purpose of the IR is to find a map between two different situation images. In this way, the main objective is to find this map to reconstruct the target image as optimum as possible.
Methods: Needless to say, the IR task is an optimization problem. As the optimization method, although the evolutionary ones are sometimes more effective in escaping the local minima, their speed is not emulated the mathematical ones at all. In this paper, we employed a mathematical framework based on the Newton method. This framework is suitable for any efficient cost function. Yet we used the sum of square difference (SSD). We also provided an effective strategy in order to avoid sticking in the local minima.
Results: The proposed newton method with SSD as a cost function expresses more decent speed and accuracy in comparison to Gradient descent and genetic algorithms methods based on presented criteria. By considering SSD as the model cost function, the proposed method is able to introduce, respectively, accurate and fast registration method which could be exploited by the relevant applications. Simulation results indicate the effectiveness of the proposed model.
Conclusion: The proposed innovative method based on the Newton optimization technique on separate cost functions is able to outperform regular Gradient descent and genetic algorithms. The presented framework is not based on any specific cost function, so any innovative cost functions could be effectively employed by our approach. Whether the objective is to reach accurate or fast results, the proposed method could be investigated accordingly.

Introduction

Image registration can be beneficial in numerous areas. There are many situations that two taken images represent the same location or object while their perspective is different [1]. They might be taken from two different angels or might be scaled in different values. As the matter of fact, recognizing the similarity between images from the mentioned situation is a cumbersome task for the machines [2]. By generating a map between two images that is capable of detecting every corresponding pixel from the first image into the target image, we are able to recognize the similarities. The goal of image registration (IR) methods is to find this map [3].

There are two main categories for IR applications. In the first category, target image is changed based on its rotation and scale values [4]. The transformation is the same for all applied pixels. The lines in the first image are still a line in the second image but with a different rotation or scale. This type of IR is called rigid registration [5], [6]. If in the target image the parallel line does not remain parallel, we face a non-rigid (or deformable) registration [7], [8]. In both methods, the target image would be constructed by an optimized transformation matrix [9]. This matrix draws a map from the first image to the second one. IR methods can work on different aspects of images to recognize the targeted map. Some rigid IR methods tend to work on the intensity value of the images; this method is called intensity-based method [7], [10]. In this method, all the criteria for judgments of registration goodness are based on the image's intensity [11]. This method is wildly used because of its simplicity and reliability [12]. Meanwhile, other rigid IR methods tend to work on special extracted features from two images and try to register the first image to the target image merely by the mentioned features [13], [14]. Due to the robustness of the intensity-based method, we favored intensity-based technique in the current study.

For finding the mentioned map as an optimization problem [15], IR methods must start with a starting values [16]. Some researchers tend to deal with the problem by the means of evolutionary computing (EC) methods [17]. There are numerous research studies in this area that have exploited the capability of ant colony algorithm [18] or swarm intelligence method [19]; and in many cases the genetic algorithm [20]. Some of the studies have also employed more innovative and hybrid methods in EC approaches to find an optimized transformation matrix [6]. These methods are widely used because of their capability to escape from local minima [19]. However, these algorithms need a considerable amount of time for finding the optimum solution for transformation matrix; in this way, they could not be wieldy applied in real time applications [21], [22]. For this reason, mathematical-based optimization algorithms might be more useful [23]. Although their application in optimization problem might be more cumbersome than EC algorithms, the speed of convergence highly favors the employment of mathematical-based optimization algorithms.

In the IR application, the primary usage of IR method is analyzing medical imaging [8], [24]-[26]. Moreover, these methods are wieldy used in geographical systems [27] and remote sensing [28]. In most of these areas, researchers attempt to exploit optimization algorithms to find the optimum transformation. Mathematical-based and evolutionary algorithms have attracted attention more than other methods [29]. However, there are several investigations that tend to employ other methods such as SIFT [28], [30], Markov random field [31], sparse representation [32] and Fuzzy-based method [20].

Mathematical optimization methods such as Gradient descent [26] and Newton methods [21] are capable of reaching near the optimum solution in considerably shorter time in comparison to EC methods. There is a relevant study [33] in which authors compared the performance of different mathematical-based optimization algorithms with working on high resolution medical imaged (CT and MRI images). Their objective function was to maximize the mutual information between the target image and the built image. In [16], authors proposed an adaptive stochastic Gradient descent (ASGD) method which is capable of adapting the step size in every iteration. Their method was run on medical images and showed enhanced performance in comparison to the similar non-adaptive methods. In [34], the authors considered a typical multiscale registration setting where the global two-dimensional translation between a pair of images is estimated by smoothing the images and minimizing the distance between them with Gradient descent. The changing parameter in their work was the translation value. In **Error! Reference source not found.**, authors mimicked the proposed method in [16] but this time on 3D medical images (MRI images). Because of excessive time consumption of 3D image registration process, they focused on the speed of convergence of their model. Based on comparisons, their proposed method is able to outperform similar methods in the case of time consumption. Alongside with Gradient descent method, its second order companion, the Newton method, absorb so many attention as well. In **Error! Reference source not found.**, authors exploited Levenberg Marquardt (L-M) and b-spline method to maximize their mutual information cost function. Their simulation based on ideal and noisy environments shows the supremacy of their method over similar methods. The mutual information as the cost function has also been considered in other works [25]. In **Error! Reference source not found.**, authors used L-M method to maximize the speed of the convergence. They attempted to accomplish a fast convergent method by optimizing the L-M step size. Their simulation on medical images has shown promising results.

In the mentioned studies, authors tried to propose much faster methods. This point underscores the important of convergence speed. Second order methods such as Newton and L-M methods can suggest improved speed. However, they need to be capable of escaping the trap of local minima. This idea suggests the importance of accuracy as well, the point that has been almost neglected in the reviewed studies. According to IR purposes, the weight of speed and accuracy importance should be adjusted. Some applications tend to reach a proper solution in the shortest time possible. In this situation, the accuracy might be compromised for the speed of the model. Some other applications need to be as accurate as possible. Here, we considered both factors and tried to fulfill their requirements. Newton method with cost function of sum of square difference (SSD) is the basis of our purposed method. However, we faced the local minima difficulty in this task. By applying a novel method, we could reach better and faster results. Instead of solving a two-variable problem, we conduct a treatment to face a single variable optimization problem in every step. We have employed root mean square error (RMSE) [31] and mutual information **Error! Reference source not found.** for evaluating the goodness (accuracy) of registration.

The content of this paper would be as follows: The second Section conveys the proposed method. In the third Section, the accomplished simulations and comprehensive comparisons is mentioned. Finally, in the fourth Section, the conclusion of the work is presented.

Proposed method

In this paper, the main intention is to minimize the SSD as the cost functions. The SSD can be defined as follows:

$$SSD = \sum_{i=1}^{n}\left(f(z_i) - g(Tz_i)\right)^2 \tag{1}$$

where Tz is $Tz = [X \quad Y] = T.z = T.[x \quad y]$ and n is number of pixels; “f” is the target image and “g” is the moving image through the iterations. The objective is to move the "g" function toward the “f” as close as possible. In other words, we intended to minimize the SSD. We employed the Newton method to solve the mentioned optimization problem. The problem in the Newton form would look like the following equation:

$$P = [s \quad \theta]^T.\, in\ Newton\ Meghod\ \Rightarrow$$

$$p^{k+1} = p^k - \lambda H^{-1}\nabla SSD \tag{2}$$

where ∇SSD(gradient of SSD) and H (Hessian matrix) would be calculated as follows:

$$\nabla \mathrm{SSD} = -2\sum_{i=1}^{n}\left(f(z_i) - g(Tz_i)\right)J\nabla g(Tz_i) \tag{3}$$

$$H = 2\sum_{i=1}^{n}\frac{\partial(g(Tz_i))}{\partial p}\frac{\partial[g(Tz_i)]}{\partial p} - 2\sum_{i=1}^{n}\left(f(z_i) - g(Tz_i)\right)\frac{\partial^2}{\partial p^2}[g(Tz_i)] \tag{4}$$

The transformation matrix of *T* is equal to:

$$T = \begin{bmatrix} s\,cos(\theta) & s\,sin(\theta) \\ -s\,sin(\theta) & s\,cos(\theta) \end{bmatrix} \tag{5}$$

where “*S*” indicates the scale value and “θ” indicates the rotation angle. This matrix is the main variable of the problem and its optimum values ought to be found. In this way, we need to access the derivation of the “*S*” and “θ”. The Jacobean of the *T* is calculated as follows:

$$J = \frac{\partial Tz}{\partial p} = \frac{\partial(T.z)}{\partial p} = \begin{bmatrix} x\,cos(\theta) + y\,sin(\theta) & -x\,sin(\theta) + y\,cos(\theta) \\ -x\,s\,sin(\theta) + y\,s\,cos(\theta) & -x\,s\,cos(\theta) - y\,s\,sin(\theta) \end{bmatrix} \tag{6}$$

In the calculation of the Hessian matrix and ∇SSD , the $\frac{\partial(g(Tz_i))}{\partial p}$ will be calculate as follow:

$$\frac{\partial[g(Tz_i)]}{\partial p} = \frac{\partial Tz_i}{\partial p}\frac{\partial[g(Tz_i)]}{\partial Tz_i} = J\nabla g(Tz_i) \tag{7}$$

The Hessian equation has a second order derivation part as $\frac{\partial^2}{\partial p^2}[g(Tz_i)]$ which equals to:

$$\frac{\partial^2}{\partial p^2}[g(Tz_i)] = \frac{\partial}{\partial p}(J.\nabla g) = \frac{\partial}{\partial p}J.\nabla g + J.\frac{\partial}{\partial p}\nabla g = \begin{bmatrix} 0 & w \\ w & ww \end{bmatrix} + \begin{bmatrix} MM & NN \\ OO & PP \end{bmatrix}.\begin{bmatrix} g_{xx} & g_{yx} \\ g_{xy} & g_{yy} \end{bmatrix} \tag{8}$$

where “g” is the gradient of the image; the indexes indicate the orientation of the derivation. For example, the g_{xx} indicates the two multiple gradient of the image in the orientation of the x axis. In the above equation, the variables would be defined as follows:

$$w = \nabla_x g.(-x\,sin(\theta) + y\,cos(\theta)) + \nabla_y g.(-x\ cos(\theta) - y\ sin(\theta)) \tag{9}$$

$$ww = \nabla_x g.(-x\,s\,cos(\theta) - y\,s\,sin(\theta)) + \nabla_y g.(x\,s\,sin(\theta) - y\,s\,cos(\theta)) \tag{10}$$

$$MM = [(x\,cos(\theta) + y\,sin(\theta))^2 + s(-x\,sin(\theta) + y\,cos(\theta))^2] \tag{11}$$

$$NN = [(x\,cos(\theta) + y\,sin(\theta))(-x\,sin(\theta) + y\,cos(\theta)) + s(-x\,sin(\theta) + y\,cos(\theta))(-x\,cos(\theta) - y\,sin(\theta))] \tag{12}$$

$$OO = \left[s\left(-x\,sin(\theta) + y\,cos(\theta)\right)\left(x\,cos(\theta) + y\,sin(\theta)\right) + s^2(-x\,cos(\theta) - y\,sin(\theta))(-x\,sin(\theta) + y\,cos(\theta))\right] \tag{13}$$

$$PP = [s(-x\,sin(\theta) + y\,cos(\theta))^2 + s^2(-x\,cos(\theta) - y\,sin(\theta))^2] \tag{14}$$

These equations build the target image properly. However, we observed in some cases that the solution is trapped in the local optimum and failed to reach the correct corresponding value of the scale and rotation. By proposing an innovative treatment, we can escape from the local optimum. We propose an interleaved method which is able to push the value of the scale and rotation to their optimum value. In this way, for a single iteration, by the assumption of the constant scale value, the rotation value would be calculated. The treatment would be reversed for the next iteration. In other words, in this stage, the rotation value presumed to be constant and the scale value would be pushed to its optimum value. Note that the content value for every parameter is decided by the calculated value in the previous iteration. Here, we introduced the equations related to constant rotation and variant scale.

$$H = \frac{\partial \nabla SSD}{\partial s} = -2\sum_{i=1}^{n} \frac{\partial(f(x_i)-g(Tx_i))}{\partial s}\frac{\partial[g(Tx_i)]}{\partial s} - 2\sum_{i=1}^{n}(f(x_i)-g(Tx_i))\frac{\partial^2}{\partial s^2}[g(Tx_i)] \quad (15)$$

$$\nabla SSD = \frac{\partial \nabla SSD}{\partial s} = 2\sum_{i=1}^{n} J_S\nabla g(Tx_i)\,J_S\nabla g(Tx_i) - 2\sum_{i=1}^{n}(f(x_i)-g(Tx_i))\frac{\partial^2}{\partial s^2}[g(Tx_i)] \quad (16)$$

$$\frac{\partial^2}{\partial s^2}[g(Tx_i)] = \frac{\partial}{\partial s}\frac{\partial Tx_i}{\partial s}\frac{\partial g(Tx_i)}{\partial Tx_i} = \frac{\partial}{\partial s}(J_S.\nabla g) = \frac{\partial}{\partial s}J_S.\nabla g + J_S.\frac{\partial}{\partial s}\nabla g \quad (17)$$

$$\frac{\partial}{\partial s}J_S = [0 \quad 0] \quad (18)$$

$$\frac{\partial^2}{\partial s^2}[g(Tx_i)] = T_S.\frac{\partial}{\partial s}\nabla g = T_S.\begin{bmatrix} x\,g_{gxx} + y\,g_{xy} \\ x\,g_{yx} + y\,g_{yy}\end{bmatrix} = x^2\,g_{gxx} + xy\,g_{xy} + yx\,g_{yx} + y^2\,g_{yy} \quad (19)$$

$$H = \frac{\partial \nabla SSD}{\partial s} = 2\sum_{i=1}^{n}(x\,gx + y\,gy)^2 - 2\sum_{i=1}^{n}(f(x_i) - g(Tx_i))(x^2\,g_{gxx} + xy\,g_{xy} + yx\,g_{yx} + y^2\,g_{yy}) \quad (20)$$

Similarly, our model based on constant scale and variant rotation could be defined as follows:

$$H = \frac{\partial \nabla SSD}{\partial p} = 2\sum_{i=1}^{n}(J_\theta \nabla g(Tx_i))^2 - 2\sum_{i=1}^{n}(f(x_i) - g(Tx_i))\frac{\partial^2}{\partial \theta^2}[g(Tx_i)] \quad (21)$$

$$J_\theta \nabla g(Tx_i) = [-x\,sin(\theta) + y\,cos(\theta) \quad -x\,cos(\theta) - y\,sin(\theta)]\begin{bmatrix} g_x \\ g_y \end{bmatrix} \quad (22)$$

$$\frac{\partial^2}{\partial \theta^2}[g(Tx_i)] = [-x\cos(\theta) - y\sin(\theta)]g_x + [x\sin(\theta) - y\ \cos(\theta)]g_y + (-x\sin(\theta) + y\cos(\theta))^2 g_{gxx} + (-x\sin(\theta) + y\cos(\theta))(-x\cos(\theta) - y\sin(\theta))g_{xy} + (-x\cos(\theta) - y\sin(\theta))(-x\sin(\theta) + y\cos(\theta))g_{gyx} + (-x\cos(\theta) - y\sin(\theta))^2 g_{yy} \quad (23)$$

In this way, we proposed an innovative treatment for finding the optimum multivariate values. By presuming the constant value for one of the rotation or scale value through the interleaved iterations, the solution can escape from local optimum and reach its global value. As a matter of fact, in this treatment, we are able to reduce the problem complexity by turning a two-variable problem into a single-variable optimization problem.

Simulation and Results

For evaluation of the proposed method, multiple simulations based on benchmark images have been done. These images have been studies numerously in the image processing literature and also are among the most famous images in the image processing field. Fig. 1 shows the images; from now on, we refer to each image by its name.

Fig. 1: Four benchmark images of this work. a: Airplane, b: Baboon, c: Fruit, d: Lena.

Our method is based on Newton method and as discussed earlier, SSD has been considered as its cost function. These cost functions could be considered for Gradient descent algorithms as well. In this way, for the first simulation, we compared the performance of Newton and Gradient descent algorithms by measuring mutual information (MI) and root mean square error (RMSE). Their equations have been defined as follows:

$$RMSE = \frac{\sum_{i=1}^{m}\sum_{j=1}^{n}(I_1(i.j) - I_2(i.j))^2}{m \times n} \quad (24)$$

where I_1 and I_2 are images, m and n are the size of images; i and j are coordinates of images.

$$MI = H(I_1) + H(I_2) - H(I_1.I_2) \quad (25)$$

$$H(I_1) = -\sum_{0}^{h} P_{I_1}.log_2(P_{I_1}) \quad (26)$$

where $H(I_1)$ and $H(I_1.I_2)$ represent entropy of I_1 and the combination of two images, respectively, and P_{I_1}

represents marginal probability distribution that can be determined by the normalized histogram of the image. Note that the higher MI and lower RMSE would be preferred.

Fig. 2 represents the first simulation which is the comparison of Newton and Gradient descent methods. Newton method has shown better results for two out of four benchmark images (Baboon and Fruit). SSD cost function has shown much more speed for convergence. Note that the rotation degree and scale value have been set to a constant value (30 and 0.7, respectively).

Newton method expresses more decent speed and accuracy in comparison to Gradient descent method based on MI and RMSE criteria. In this way, Fig. 2 suggests the priority of Newton method over Gradient descent for the two studied images (Baboon and Fruit).

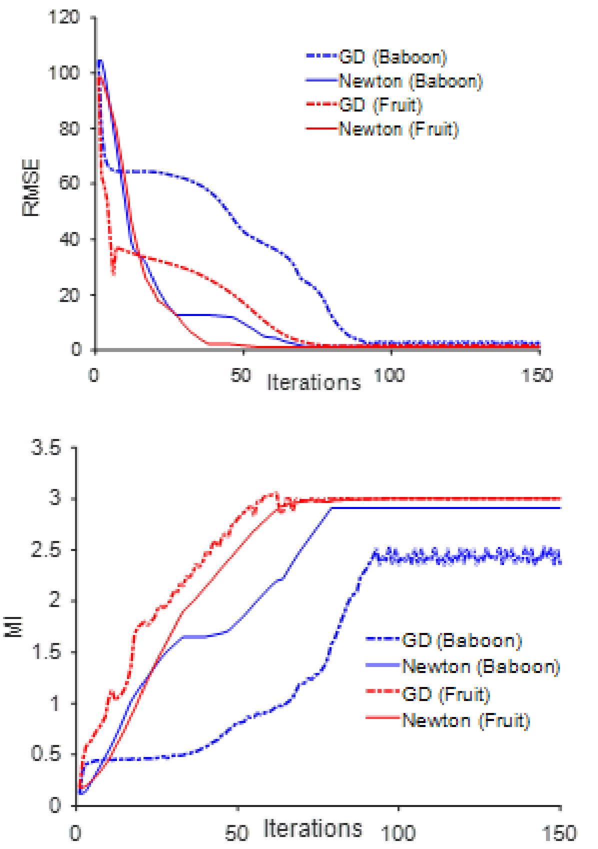

Fig. 2: Comparison of Newton and Gradient descent (GD) methods. a: Comparison of two methods based on SSD as the cost function in the case of RMSE value, b: Same comparison as an in the case of MI value.

The mentioned priority of Newton method could not happen in all simulations. Fig. 3 represents the best outcome of each method after 200 iterations. This analysis has been run on all benchmark images. Based on 20 runs on every condition, results in Fig. 3 have been extracted. Note that in every run, the starting point has been chosen randomly. Both criteria favor Newton over GD based on Baboon and Fruit images. This advantage is reversed in Lena and Airplane pictures; best results for this images belong to GD simulations. This observation in our simulation encouraged us to alter the Newton method application to reach enhanced results.

As it has been discussed earlier, we applied a modification to the application of the Newton method. In this case, we considered the value of the scale parameter as a constant value and iterate the algorithm heading toward optimum rotation parameter. In the succeeding iteration, the treatment would be reversed in favor of finding optimal scale parameter. The results of the simulation in our proposed method show superior performances in both cost functions and criteria.

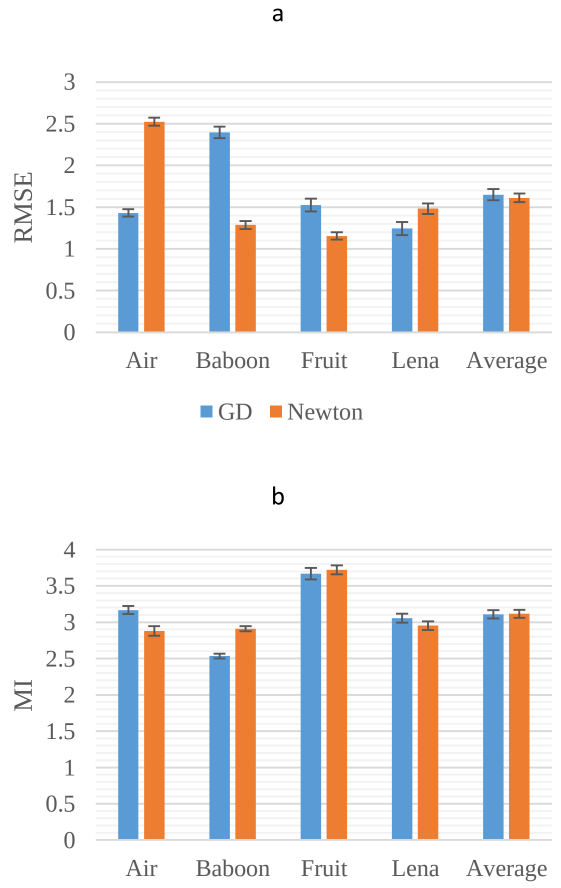

Fig. 3: Comparison of the best solution between SSD-based methods a: Comparison has been done based on the RMSE criterion, b: Compression has been done based on MI criterion. Error bars are standard deviations.

The mentioned practice enables the model to become more efficient in escaping from local minima. Since this practice introduces just one variable by each iteration, the problem space is much simpler than two-dimension space. In this way, we expect to have less problem with local minima. This problem could be readily exacerbated by the Newton method; since the newton method deals with the second order derivation – a more complex space. The initial results confirm this phenomenon.

This observation in our simulation encouraged us to alter the Newton method application to reach enhanced results. In fact, two less performed images is trapped in the local minima. The major question is whether the proposed method can enable the model to outperform GD.

Based on the simulations in Fig. 2 and 3, GD is able to produce more enhanced results in comparison to the Newton method on other two images (Lena, Airplane). However, Fig. 4 expresses the supremacy performance of the proposed method to GD based on two mentioned images. Both criteria confirm the improved results of the proposed method. Similar to Fig. 2, SSD has led to fast and accurate convergence.

a

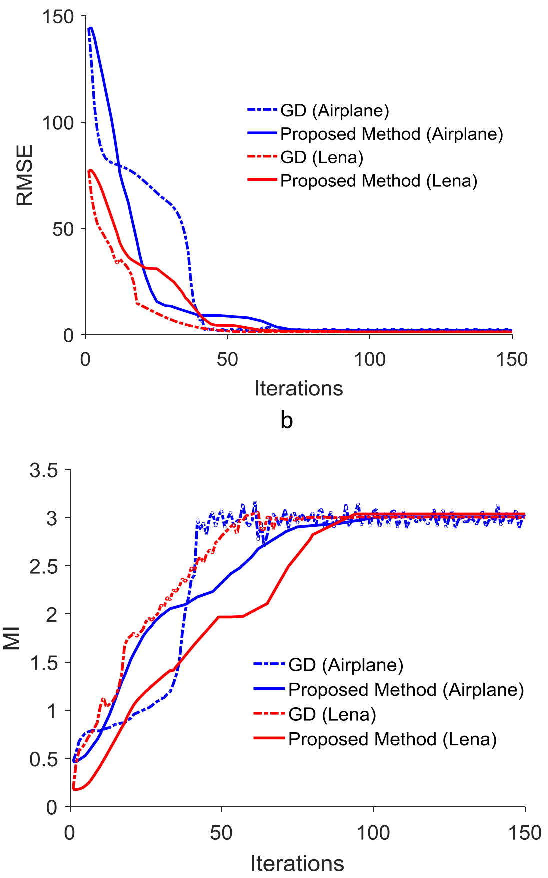

Fig. 4: Comparison of GD and the proposed method. a: Comparison of two SSD-based methods as the cost function in the case of RMSE value, b: Same comparison as (a) in the case of MI value.

Furthermore, we simulated the proposed method on two images in Fig. 2 (Baboon, Fruit). Having 20-run simulations, results for every condition and criterion have been extracted and assembled in Fig. 5. Results in Fig. 5 indicate that the proposed method is able to perform better in comparison to GD. In average, the proposed method easily outperforms the GD. This means that the idea of interleaved variables is working properly. Note that various results in every run are caused by the various starting point in 200 iterations (same as Fig. 3).

All the made simulations so far have been accomplished on a certain scale and degree values (0.7 and 30, respectively). It is vital to evaluate the proposed method on different parameters and compare the outcomes with GD algorithm. It is necessary for a robust method to be capable of performing decently on the values of different parameters as well.

a

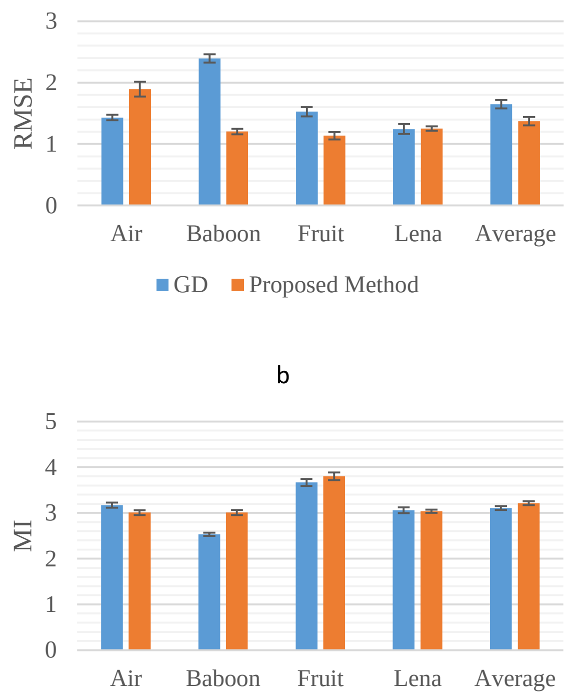

Fig. 5: Comparison of the best solution between SSD-based methods. a: Comparison has been done based on RMSE criterion, b: Compression has been done based on MI criterion. Error bars are standard deviations.

Fig. 6 depicts the best results of averages of four images in every criterion. We have considered 4 different values for scale and rotation which generate 16 different conditions.

Almost in every condition, the proposed method outperforms GD.

Considering both criteria, the proposed method based on SSD shows better performance. This order has been preserved for GD simulations as well.

Because of the wider available range in RMSE (Fig. 6.a), this criterion is able to recognize more discrimination between different methods in various conditions.

The presented results in Fig. 6 endorse the capability and robustness of the proposed method in different scales and rotation conditions. By considering SSD as the model cost function, the proposed method is able to introduce, respectively, accurate and fast registration method which could be exploited by the relevant applications.

a

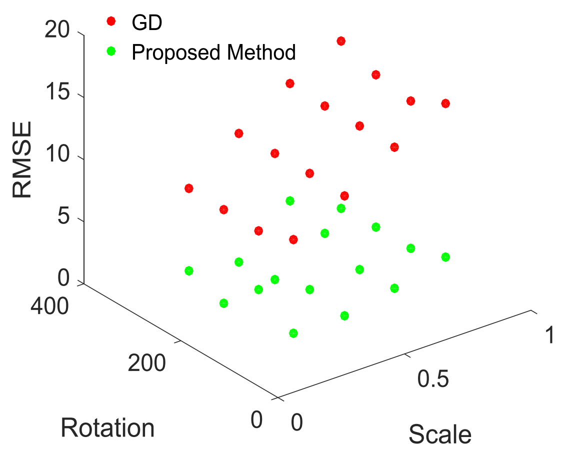

b

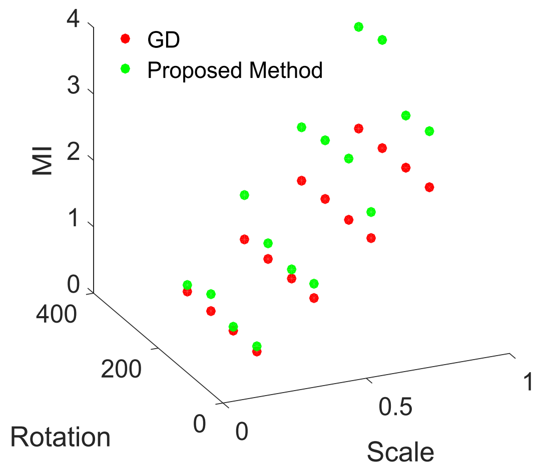

Fig. 6: Comparison of GD and the proposed method on various parameters by different criteria. a: Comparison of the proposed method and GD performance, based on SSD cost functions by RMSE criterion, b: Same analysis as a for MI criterion.

We also compared our proposed method with one of the most famous EC methods, GA. For more extensive comparison, we considered four more images in our analysis.

As it has been shown in Table 1, in both criteria, the proposed method outperforms the GA and GD. Note, the analysis in Table 1 have been done similar to Fig. 6. In other words, for each image, we calculated the results of each image in any 16 conditions (4 variant scales and 4 variant rotation). Average of these values have been presented in Table 1. Accordingly, the proposed method is able to perform superior to GA and GD.

Table 1: Comparison of our Method with GA and GD.

	RSME			MI		
Images	**GD**	**GA**	**Our Method**	**GD**	**GA**	**Our Method**
Lena	10.11	9.5	**1.45**	1.88	1.89	**2.95**
Airplane	9.78	5.89	**1.78**	2.08	2.45	**2.9**
Baboon	14.42	3.45	**2.01**	1.1	2.55	**2.72**
Fruit	9.87	14.5	**1.89**	1.32	1.28	**3.12**
Cameraman	8.66	12.78	**0.98**	1.98	1.12	**3.25**
Barbara	7.1	9.84	**2.1**	2.33	1.42	**1.88**
Boat	12.8	9.1	**1.47**	1.4	1.41	**1.78**
House	11.3	12.5	**1.16**	1.42	1.21	**1.89**
Average	10.50	9.69	**1.60**	1.68	1.66	**2.56**

Conclusion

This paper proposed an innovative method based on the Newton optimization technique on separate cost functions. Both cost functions have been optimized by means of the proposed method. As a matter of fact, the proposed method is able to outperform regular Gradient descent and Newton simulations based on MI and RMSE criteria. In our intensity-based rigid resignation, there are two parameters, namely, rotation and scale values.

Through the iterations, we have set one variable to a constant value and attempted to optimize the other one by setting it free. Free and constant parameters have been replaced constantly through the path of reaching the final solution. In fact, we altered the two-variable optimization problem into the single-variable one. The temporary simplified single-variable problem is able to search the problem space more easily and effectively. More capable of escaping from local minima, this treatment helps the registration to be faster and more precise.

Furthermore, we conducted a simulation whose rotation and angle of the target image were analyzed by various values (Fig. 6). Using this simulation, the authors are able to confirm the robustness and enhanced performance of our proposed methods in comparison to Gradient descent. The speed and accuracy of SSD as the cost functions could be exploited in a combined cost function which potentially can promise enhanced performance.

Since our framework is not based on any specific cost function, some innovative cost functions could be effectively employed by our approach. Whether the objective is to reach accurate or fast results, the proposed method could be investigated accordingly.

Author Contributions

M. S. Esfand abadi and R. ebrahimpour designed the type of experiment and suggested how to display them graphically. They also analyzed the data concluded.

J. Khosravi extracted the formulas, implemented codes, and simulated experiments.

Acknowledgment

We sincerely thank M. Saadatmand-Tarzjan for presenting the gradient method jointly with J. Khosravi [26]. The method presented in this article was compared with the mentioned method. However, the objective function defined there is different.

Conflict of Interest

The authors declare that there is no conflict of interests regarding the publication of this manuscript. In addition, the ethical issues, including plagiarism, informed consent, misconduct, data fabrication and/or falsification, double publication and/or submission, and redundancy have been completely observed by the authors.

Abbreviations

SSD	Sum of square difference
H	Hessian matrix
λ	Convergence parameter
F(x)	Fixed image
G(x)	Moving image
∇	Gradient
J	Jacobian matrix
∇_x	Gradient in x direction
S	Image Scale
θ	Image angle

References

[1] J. Fan, X. Cao, P.-T. Yap, D. Shen, “BIRNet: Brain image registration using dual-supervised fully convolutional networks,” Med. Image Anal., 54: 193–206, 2019.

[2] M. Moradi, M. Sadeghi, “Combining and steganography of 3-D face textures,” J. Electr. Comput. Eng. Innov., 5(2): 93–100, 2017.

[3] R. Nain, N. Kumar, “Medical image registration by GSA optimized matching algorithm,” Int. J. Curr. Eng. Technol., 6(2): 472–476, 2016.

[4] Z. Xu et al., “Rigid motion correction for magnetic resonance fingerprinting with sliding-window reconstruction and image registration,” Magn. Reson. Imaging, 57: 303–312, 2019.

[5] G. C. S. Ruppert et al., “Medical image registration based on watershed transform from greyscale marker and multi-scale parameter search,” Comput. Methods Biomech. Biomed. Eng. Imaging Vis., 5(2): 138–156, 2017.

[6] R. Panda, S. Agrawal, M. Sahoo, R. Nayak, “A novel evolutionary rigid body docking algorithm for medical image registration,” Swarm EComput., 33): 108–118, 2017.

[7] B. Haghighi, N. D. Ellingwood, Y. Yin, E. A. Hoffman, C. L. Lin, “A GPU-based symmetric non-rigid image registration method in human lung,” Med. Biol. Eng. Comput., 56(3): 355–371, 2018.

[8] A. Sotiras, C. Davatzikos, N. Paragios, “Deformable medical image registration: a survey,” IEEE Trans. Med. Imaging, 32(7): 1153–1190, 2013.

[9] H. Yu et al., “Learning 3D non-rigid deformation based on an unsupervised deep learning for PET/CT image registration,” presented at The Biomedical Applications in Molecular, Structural, and Functional Imaging, California, United States, 2019.

[10] A. Valsecchi, S. Damas, J. Santamaria, “Evolutionary intensity-based medical image registration: a review,” Curr. Med. Imaging Rev., 9(4): 283–297, 2014.

[11] E. Castillo, “Quadratic penalty method for intensity-based deformable image registration and 4DCT lung motion recovery,” Med. Phys., 46(5): 2194–2203, 2019.

[12] L. Han, H. Dong, J. R. McClelland, L. Han, D. J. Hawkes, D. C. Barratt, “A hybrid patient-specific biomechanical model based image registration method for the motion estimation of lungs,” Med. Image Anal., 39: 87–100, 2017.

[13] O. Lobachev, C. Ulrich, B. S. Steiniger, V. Wilhelmi, V. Stachniss, M. Guthe, “Feature-based multi-resolution registration of immunostained serial sections,” Med. Image Anal., 35: 288–302, 2017.

[14] J. Li, Q. Hu, M. Ai, “Robust feature matching for remote sensing image registration based on LQ-estimator,” IEEE Geosci. Remote Sens. Lett., 13(12): 1989–1993, 2016.

[15] S. Klein, J. P. W. Pluim, M. Staring, M. A. Viergever, “Adaptive stochastic gradient descent optimisation for image registration,” Int. J. Comput. Vis., 81(3): 227–239, 2009.

[16] Y. Wu, W. Ma, Q. Miao, S. Wang, “Multimodal continuous ant colony optimization for multisensor remote sensing image registration with local search,” Swarm and Evolutionary Computation, 47): 89-95, 2019.

[17] H. Ismkhan, “Effective heuristics for ant colony optimization to handle large-scale problems,” Swarm EComput., 32): 140–149, 2017.

[18] F. Ayatollahi, S. B. Shokouhi, A. Ayatollahi, “A new hybrid particle swarm optimization for multimodal brain image registration,” J. Biomed. Sci. Eng., 05(04): 153–161, 2012.

[19] I. Behravan, SH. Zahiri, SM. Razavi, "Clustering a Big Mobility Dataset Using an Automatic Swarm Intelligence-Based Clustering Method," J. Electr. Comput. Eng. Innov., 6(2): 243-261, 2019.

[20] S. Elhag, A. Fernández, A. Bawakid, S. Alshomrani, F. Herrera, “On the combination of genetic fuzzy systems and pairwise learning for improving detection rates on Intrusion Detection Systems,” Expert Syst. Appl., 42(1): 193–202, 2015.

[21] A. Mang, G. Biros, “A semi-Lagrangian two-level preconditioned Newton-Krylov solver for constrained diffeomorphic image registration,” SIAM J. Sci. Comput., 39(6): B1064–B1101, 2017.

[22] S. Ying, D. Li, B. Xiao, Y. Peng, S. Du, M. Xu, “Nonlinear image registration with bidirectional metric and reciprocal regularization,” PLoS One, 12(2): 1–19, 2017.

[23] K. Chen, G. N. Grapiglia, J. Yuan, D. Zhang, “Improved optimization methods for image registration problems,” Numer. Algorithms, 80(2): 305–336, 2019.

[24] E. Ferrante, N. Paragios, “Slice-to-volume medical image registration: A survey,” Med. Image Anal., 39): 101–123, 2017.

[25] S. Klein, M. Staring, J. P. W. Pluim, “Evaluation of optimization methods for nonrigid medical image registration using mutual information and b-splines,” IEEE Trans. Image Process., 16(12): 2879–2890, 2007.

[26] S. Etemadi, M. Saadatmand-Tarzjan, M. Shamirzaei, J. Khosravi, "An efficient 3D gradient-based algorithm for medical image registration using correlation-coefficient maximization," in Proc. 4th International Conference on Computer and Knowledge Engineering (ICCKE): 663–668, 2014.

[27] J. Le Moigne, W. J. Campbell, R. F. Cromp, "An automated parallel image registration technique based on the correlation of wavelet features," IEEE Trans. Geosci. Remote Sens., 40(8): 1849–1864, 2002.

[28] K. Yang, A. Pan, Y. Yang, S. Zhang, S. Ong, H. Tang, "Remote sensing image registration using multiple image features," Remote Sens., 9(6, p. 581, 2017.

[29] Y. Qiao, B. P. F. Lelieveldt, M. Staring, "An efficient preconditioner for stochastic gradient descent optimization of image registration," IEEE Trans. Med. Imaging, 9: 10–19, 2019.

[30] J. Zhang, G. Chen, Z. Jia, "An image stitching algorithm based on histogram matching and sift algorithm," Int. J. Pattern Recognit. Artif. Intell., 31(04): 1754006-2–14, 2017.

[31] H. Jagadish, J. Prakash, "Adaptive Markov random field model for area based image registration and change detection," Int. J. Appl. or Innov. Eng. Manag., 6(4): 50–58, 2017.

[32] Y. Li, C. Chen, Fei Yang, J. Huang, "Deep sparse representation for robust image registration," in Proc. 2015 IEEE Conference on Computer Vision and Pattern Recognition (CVPR): 4894–4901, 2015.

[33] F. Maes, D. Vandermeulen, P. Suetens, "Comparative evaluation of multiresolution optimization strategies for multimodality image registration by maximization of mutual information," Med. Image Anal., 3(4): 373–386, 1999.

[34] E. Vural, P. Frossard, "Analysis of descent-based image registration," SIAM J. Imaging Sci., 6(4): 2310–2349, 2013.

[35] Y. Qiao, B. van Lew, B. P. F. Lelieveldt, M. Staring, "Fast automatic step size estimation for gradient descent optimization of image registration," IEEE Trans. Med. Imaging, 35(2): 391–403, 2016.

[36] M. Unser, P. Thevenaz, "Optimization of mutual information for multiresolution image registration," IEEE Trans. Image Process., 9(12): 2083–2099, 2000.

[37] J. Dong, K. Lu, J. Xue, S. Dai, R. Zhai, W. Pan, "Accelerated nonrigid image registration using improved Levenberg–Marquardt method," Inf. Sci. (Ny)., 423): 66–79, 2018.

Biographies

Javanshir Khosravi is a Ph.D. student of Electrical Engineering in Shahid Rajaee Teacher Training University, Tehran, Iran. He has mastered Electronic Engineering at Shahid Beheshti University in Tehran in 2007. His field of work is Image Registration and has done research on this topic. He is interested in image processing, especially the Image Registration and Image Segmentation, and is working on this topic at the Ph.D. period and started writing the articles in this field of research.

Mohammad Shams Esfand-Abadi received the B.Sc. degree in Electrical Engineering from Mazandaran University, Mazandaran, Iran and the M.Sc. degree in Electrical Engineering from Tarbiat Modares University, Tehran, Iran in 2000 and 2002, respectively, and the Ph.D. degree in Biomedical Engineering from Tarbiat Modares University, Tehran, Iran in 2007. Since 2004, he has been with the Department of Electrical Engineering, Shahid Rajaee Teacher Training University, Tehran, Iran, where he is currently an associate professor. His research interests include digital filter theory, adaptive distributed networks, and adaptive signal processing algorithms.

Reza Ebrahimpour is a professor at the department of Computer Engineering, Shahid Rajaee Teacher Training University, Tehran, Iran. He obtained Ph.D. degree in the field of Cognitive Neuroscience from the SCS, IPM, Tehran, Iran in July 2007. Prof. Ebrahimpour is the author or co-author of more than 100 international journal and conference publications in his research areas, which include Cognitive and Systems Neuroscience, Human and Machine Vision, Decision Making and Object Recognition.

How to cite this paper:

J. Khosravi, M. Shams EsfandAbadi, R. Ebrahimpour, "Image registration based on sum of square difference cost function," Journal of Electrical and Computer Engineering Innovations, 6(2): 273-281, 2018.

DOI: 10.22061/JECEI.2019.5544.235

URL: http://jecei.sru.ac.ir/article_1138.html